

Combining Stochastic Defenses to Resist Gradient Inversion: An Ablation Study

Daniel Scheliga^a, Patrick Mäder^{a,b} and Marco Seeland^a

^aDepartment of Computer Science and Automation, Data-intensive Systems and Visualization Group (dAI.SY), Technische Universität Ilmenau, Ilmenau, Germany

^bFaculty of Biological Sciences, Friedrich Schiller University, Jena, Germany

ARTICLE HISTORY

Compiled December 6, 2024

ABSTRACT

Gradient Inversion (GI) attacks are a ubiquitous threat in Federated Learning (FL) as they exploit gradient leakage to reconstruct supposedly private training data. Common defense mechanisms such as Differential Privacy (DP) or stochastic Privacy Modules (PMs) introduce randomness during gradient computation to prevent such attacks. However, we pose that if an attacker effectively mimics a client's stochastic gradient computation, the attacker can circumvent the defense and reconstruct clients' private training data. This paper introduces several targeted GI attacks that leverage this principle to bypass common defense mechanisms. As a result, we demonstrate that no individual defense provides sufficient privacy protection. To address this issue, we propose to combine multiple defenses. We conduct an extensive ablation study to evaluate the influence of various combinations of defenses on privacy protection and model utility. We observe that only the combination of DP and a stochastic PM was sufficient to decrease the Attack Success Rate (ASR) from 100% to 0%, thus preserving privacy. Moreover, we found that this combination of defenses consistently achieves the best trade-off between privacy and model utility.

KEYWORDS

Gradient Leakage, Gradient Inversion Attack, Data Privacy, Federated Learning, Deep Learning

1. Introduction

Federated Learning (FL) leverages distributed data to collaboratively improve the utility of neural networks. Multiple clients exchange local training gradients to collaboratively train a common global model. This eliminates the need for centrally aggregated or shared data. Because training data remains local to each participating client, such collaborative learning systems aim to systematically mitigate privacy risks (McMahan et al. 2017a; Kairouz et al. 2021). However, potentially sensitive information can be reconstructed from the exchanged gradient information, thereby compromising client privacy. Iterative Gradient Inversion (GI) attacks are particularly advanced in this context (Zhu et al. 2019; Zhao et al. 2020; Wei et al. 2020; Geiping et al. 2020; Yin et al. 2021). These attacks optimize initially random dummy data to minimize a distance function between dummy gradients and the attacked client's gradients. As a result,

Corresponding author: Marco Seeland. Email: marco.seeland@tu-ilmenau.de

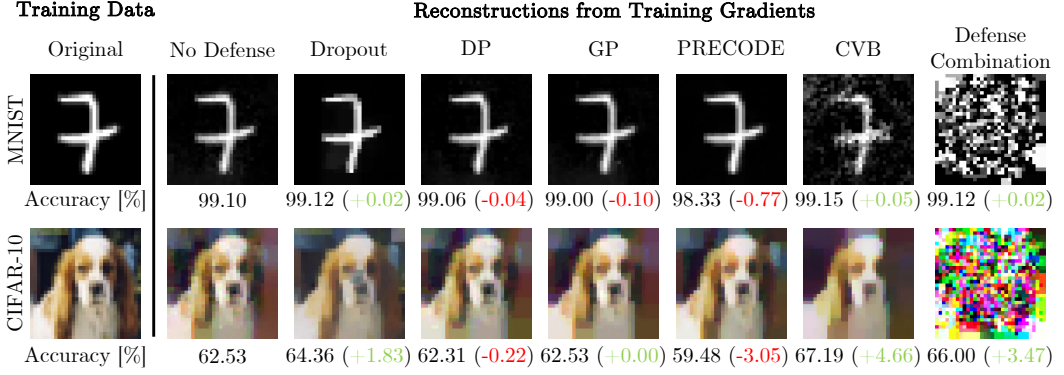


Figure 1. Visual summary of this paper: Neural networks are trained on MNIST, CIFAR-10, and four other datasets in a FL scenario. If defenses are applied on their own, they can be bypassed by targeted attacks or require such high gradient perturbation rates, that the resulting model would suffer from severe losses in model utility. However, applying a combination of defense mechanisms can prevent leakage from targeted GI attacks and even improve model utility compared to an unprotected baseline model.

they can achieve close to perfect reconstructions of the clients’ training data.

The de-facto standard defense against such privacy leaks is to perturb the exchanged gradients by applying Differential Privacy (DP) or Gradient Pruning (GP) (Bonawitz et al. 2017; Jayaraman et al. 2019; Zhu et al. 2019; Sattler et al. 2019; Jin et al. 2020; Wei et al. 2021; Ponomareva et al. 2023). However, gradient perturbation results in an inherent trade-off between model utility and privacy (Dwork et al. 2014; Jayaraman et al. 2019; Scheliga et al. 2022; Huang et al. 2021; Ponomareva et al. 2023). To avoid this trade-off, Privacy Modules (PMs) such as PRIVacy EnhancIng mODuLE (PRECODE) (Scheliga et al. 2022) and Convolutional Variational Bottlenecks (CVBs) (Scheliga et al. 2024b) have been proposed. Related work has found that Dropout has similar privacy preserving effects due to its stochasticity during training (Scheliga et al. 2023).

To test the limits of these commonly applied defense mechanisms, we adopt the perspective of an attacker. Recent work on a Dropout Inversion Attack (DIA) shows that an attacker can bypass the privacy preserving effects of Dropout by approximating the Dropout masks used by the clients during local training (Scheliga et al. 2023). Based on this observation, we argue that training data can be reconstructed even from protected gradients if the attacker sufficiently mimics the clients’ stochastic gradient computation processes. By applying this attack principle to other defenses, we identify new vulnerabilities in common defense mechanisms in general. Specifically, we propose targeted GI attacks against DP (Abadi et al. 2016), GP (Lin et al. 2017) and two variational modeling based PMs: PRECODE (Scheliga et al. 2022) and CVB (Scheliga et al. 2024b). By approximating and mimicking the client’s stochastic gradient computation behavior, these targeted attacks significantly improve the Attack Success Rate (ASR). As a result, we observe that an isolated defense mechanism cannot sufficiently protect the data from reconstruction.

To address this privacy issue, we propose to combine multiple defense mechanisms. Since each defense mechanism introduces a different type of stochasticity into the training process, the complexity of GI attacks increases, making it harder for the attacker to mimic the gradient computation process. To rigorously test the effectiveness of various defense combinations, we introduce the *Combined Defenses Inversion Attack (CDIA)*, a GI attack that is aware of the defense mechanisms employed by the client

during local training and specifically targets each defense in the attack. An extensive ablation study of defense combinations shows that combining low-level noise DP with a PM (PRECODE or CVB) is essential to protect client privacy and reduce the ASR to 0%. Moreover, this combination often results in the highest model utility compared to other defense combinations and the unprotected baseline model.

Figure 1 presents a visual summary of this paper. The specific contributions of this paper can be summarized as follows:

- We investigate four different defense techniques, namely DP, GP, PRECODE, and CVB, to analyze differences in the gradient computation process and the resulting gradients between client and attacker.
- We introduce three novel GI attacks, i.e., Differential Privacy Inversion Attack (DPIA), Gradient Pruning Inversion Attack (GPIA), and Variational Bottleneck Inversion Attack (VBIA), that specifically target these defense mechanisms by approximating and mimicking the client’s gradient computation behavior.
- We systematically combine defense techniques and perform an empirical ablation study using our proposed Combined Defenses Inversion Attack (CDIA).

2. Related Work

2.1. Attacks

Various studies have demonstrated that FL is vulnerable to security and privacy threats (Mothukuri et al. 2021; Rodríguez-Barroso et al. 2023; Rao et al. 2024; Sharma et al. 2024). This paper specifically considers GI attacks. This privacy threat is of particular interest, because attackers can achieve almost perfect reconstruction of clients’ training data from the gradient information that is exchanged during collaborative training (Zhu et al. 2019; Geiping et al. 2020; Wei et al. 2020; Rodríguez-Barroso et al. 2023). Recent work on GI attacks discusses malicious threat models that actively interfere with the training process to create favorable conditions for the GI attack (Fowl et al. 2021; Fowl et al. 2022; Wen et al. 2022; Boenisch et al. 2023). However, clients could detect such malicious behavior and stop participation in training (Boenisch et al. 2023; Garov et al. 2023). Therefore, this work focuses on the honest-but-curious server threat model, which will be discussed in more detail in Section 3.2. GI attacks can be further categorized into analytical/recursive GI attacks and iterative ones. The authors of (Aono et al. 2017; Geiping et al. 2020) show that the input to any fully connected layer in a neural network can be analytically reconstructed using the layer’s bias values. Recursive GI attacks extend analytical attacks to models that use more than one fully connected layer and get rid of the dependency on the bias term for reconstruction (Zhu et al. 2021). However these attacks are not very successful for larger batch sizes, since only the average of multiple inputs will be recovered.

Iterative GI attacks solve an optimization problem to minimize a distance function between dummy gradients and the attacked client gradients. The dummy data is iteratively adjusted to fit the client gradients. As a result, the optimized dummy data resembles the client’s private training data (Zhu et al. 2019; Zhao et al. 2020; Wei et al. 2020; Geiping et al. 2020). Section 3.3 will explain how these attacks work in more detail. Most research on GI attacks proposes some adjustments to some of the attack components to slightly increase the quality of the reconstructed data, stabilize the attack optimization process and/or increase the convergence speed (Wang et al. 2020; Jeon et al. 2021; Yin et al. 2021). Recent work also applies generative modeling

to increase the fidelity of reconstructions (Jeon et al. 2021; Ren et al. 2022; Xu et al. 2022; Li et al. 2022; Zhang et al. 2023; Fang et al. 2023). However, they often require additional knowledge on the training data distribution of the victim client and auxiliary data. Furthermore, although the reconstructions do represent the victim clients training data distribution they might be sufficiently different from the actual training data. For a more detailed overview of the field of GI, we refer interested readers to several survey papers (Zhang et al. 2022; Yang et al. 2023; Li et al. 2023).

2.2. *Defenses*

A comprehensive analysis of privacy leakage via GI attacks identified relevant parameters that affect the severity of privacy leakage and potential mitigation strategies (Wei et al. 2020). They found that batch size, image resolution, choice of activation functions, and the number of local iterations before gradient exchange can impact privacy leakage. Supporting findings are reported in (Zhu et al. 2019; Geiping et al. 2020; Zhao et al. 2020; Zhu et al. 2021; Pan et al. 2022). While such parameters and training conditions are certainly relevant and can be carefully selected to prevent attacks, they do not guarantee the protection of sensitive data from GI attacks. In fact, Geiping et al. demonstrated successful attacks on deep neural networks, e.g., ResNet-152, trained for multiple communication rounds and even for batches of 100 images. Moreover, parameter selection is often influenced by other factors, such as hardware limitations. Hence, to achieve data privacy, defense mechanisms should be actively developed, analyzed, and applied.

Gradient Pruning (GP)

GP is the de-facto standard to defend against privacy leakage in collaborative learning scenarios (Kairouz et al. 2021). The two most common general approaches are gradient compression and noisy gradients. Gradient compression is primarily used to reduce communication costs and memory usage during collaborative training. Since compression mechanisms reduce the entropy of the gradients, they also decrease the success of GI attacks. This can be achieved with GP (Lin et al. 2017; Tsuzuku et al. 2018; Deng et al. 2020), by removing the least relevant information from the training gradients before sending them to the server. Most state-of-the-art methods utilize noisy gradients to guarantee a provable degree of privacy for clients in collaborative training (Bonawitz et al. 2017; McMahan et al. 2017b; McMahan et al. 2018; Li et al. 2019). The concept of using noise to limit the information disclosure about individuals was originally introduced in the field of DP (Abadi et al. 2016; Dwork et al. 2014). In practice, Gaussian or Laplace noise is added to the gradients before their exchange. Although added noise can suppress GI attacks, it also negatively impacts both the training process and the final model utility. Furthermore, it remains unclear how much privacy can actually be guaranteed in practical scenarios. Recent work demonstrates that the theoretical privacy guarantees of DP do not necessarily ensure practical privacy (Wang et al. 2022). In general, all gradient perturbation methods exhibit a well-observed side effect: an inherent trade-off between model utility and privacy (Dwork et al. 2014; Jayaraman et al. 2019; Zhu et al. 2019; Wei et al. 2020; Huang et al. 2021). While the use of more training data might mitigate such drops in model utility (Dwork et al. 2014), this is often not feasible in practical scenarios.

Privacy Module (PM)

The authors of (Scheliga et al. 2022) propose to extend neural network architectures

with PM. Such modules can be generically integrated into any existing model architecture without requiring further model modifications. More importantly, Privacy Module (PM)s shall not notably harm the final model utility or training process, e.g., by causing increased convergence times. The authors proposed PRECODE as first realization of a PM. PRECODE is implemented as Variational Bottleneck (VB) that uses stochastic sampling to generate a stochastic latent representation of the training data, which is then used to calculate the model prediction. While the model retains feature information that is relevant to solving the models original task, gradients are computed based on stochastic feature representations instead of deterministic ones. Stochastic feature representations are randomly sampled in each optimization step, which counters iterative GI attacks by design. Recent work has identified severe weaknesses in PRECODE’s use of fully connected layers and propose a Convolutional Variational Bottleneck (CVB) as novel PM that uses only convolutional layers for variational modeling (Scheliga et al. 2024b). Similar to PRECODE, the CVB protects against GI attacks through stochastic sampling. Due to the local connectivity of convolutional layers, the CVB also requires considerably less additional parameters. This allows for notable reduction of computational and communication costs while effectively preserving privacy. An extensive experimental evaluation shows that, compared to other defense mechanisms, CVB offers the best trade-off between model utility and privacy in a broad set of scenarios.

Dropout

A simple and effective method to implement stochastic sampling without additional model parameters is Dropout. Dropout is a regularization technique used to reduce overfitting in neural networks (Hanson 1990; Hinton et al. 2012). While Dropout can enhance the performance of models (Srivastava et al. 2014), recent studies suggest it can also protect shared gradients from GI attacks (Wei et al. 2020). However, recent work systematically disseminates Dropout as defense and expose new vulnerabilities (Scheliga et al. 2023). They show that an attacker can sufficiently approximate and mimic the stochastic training behavior of the client to effectively bypass the protection seemingly induced by Dropout.

3. Preliminaries

3.1. Federated Learning

This paper investigates the privacy of FL processes (McMahan et al. 2017a; Kairouz et al. 2021). Instead of training one model on a centralized dataset, in FL multiple clients collaborate to train a common global model. Each client has their own private local training dataset. A centralized orchestration server S coordinates the collaborative training process. Clients initialize their local model from a given global model state. After a defined number of local training steps, clients return their local model updates, i.e., their model gradients G to the server. Hence, training data does not have to be shared and remains local with each client. The server updates the global model state by aggregating the client’s local model updates. For example, Federated Averaging (FedAvg) implements this aggregation using a simple weighted average of the updated states (McMahan et al. 2017a). This process is repeated iteratively until convergence or some other termination criterion is satisfied. In terms of privacy, all collaborative training approaches that are based on the exchange of gradient information suffer from similar vulnerabilities, e.g., peer-to-peer or cluster-based collaborative training (Roy

et al. 2019; Duan et al. 2019; Scheliga et al. 2024a).

3.2. Threat Model

Based on the threat model taxonomy in (Wagner et al. 2018) and consistent with related work on GI attacks (Zhu et al. 2019; Geiping et al. 2020; Wei et al. 2020; Scheliga et al. 2024b; Rodríguez-Barroso et al. 2023), we adopt a *honest-but-curious server* threat model. In this threat model, attackers are *curious* as they apply GI attacks to reconstruct potentially sensitive training data from exchanged gradients. They act *locally* and *internally* on a restricted part of the system, i.e., the orchestration server S . Attackers are *passive*, i.e., they only read and observe exchanged information, e.g., model parameters/gradients. This passive behavior is also referred to as *honest*, since there is no active interference with the training process. Consistent with an orchestration server in FL scenarios, attackers have *white-box* access to the model and *prior knowledge* on the used training protocols. Specifically this includes the model F , the model weights W , the training loss function \mathcal{L} , and the exchanged gradients $G = \nabla \mathcal{L}_W(F(x), y)$ of the attacked victim client.

3.3. Gradient Inversion Attacks

Gradient Inversion (GI) attacks aim to reconstruct the training data (x, y) of a victim client C that was used during a local training step of FL. GI attacks aim to solve the following optimization problem:

$$\arg \min_{(x', y')} \text{GDF}(\nabla \mathcal{L}_W(F(x), y), \nabla \mathcal{L}_W(F(x'), y')) + \mathcal{R}. \quad (1)$$

Here x refers to the victim clients' input data and y to the associated ground truth output label. F is the attacked model with parameters W and \mathcal{L}_W defines the model objective function. The attack optimization procedure aims to find some dummy data (x', y') that results in similar gradients as the victim clients' data. The gradient $G = \nabla \mathcal{L}_W(F(x), y)$ denotes the *victim gradient* that is computed using client training data, whereas $G' = \nabla \mathcal{L}_W(F(x'), y')$ is the *dummy gradient* that is computed with dummy data. \mathcal{R} represents a regularization scheme that aims to improve the reconstruction and stabilize the attack optimization process. The general working principle of iterative GI attacks is formalized in Algorithm 1.

First the attacker initializes some in- and output dummy data (x', y') . The dummy data is typically initialized randomly from a Normal distribution $\mathcal{N}(0, \mathcal{I})$. The attacker iteratively updates the dummy data via gradient descent to minimize a Gradient Distance Function (GDF) between the victim gradient G and the dummy gradient G' . The most commonly used distance functions are the Euclidean and cosine distance. The attack optimization ends, if a pre-defined termination criterion is reached, e.g., a maximum number of iterations or a gradient distance threshold. Optimization is typically performed using gradient descent with L-BFGS (Liu et al. 1989) or Adam (Kingma et al. 2014) optimizers.

The first proposed iterative GI attack, *Deep Leakage from Gradients* (DLG), uses Euclidean distance as GDF, no regularization scheme and L-BFGS as optimizer (Zhu et al. 2019). The attack is mainly limited to the reconstruction of training data from very small batches. Larger batches make the attack optimization process unstable

Algorithm 1 General Gradient Inversion (GI) Attack

Input: F : neural network; \mathcal{L} : training loss function; GDF: gradient distance function;

$G = \nabla \mathcal{L}_W(F(x), y)$: victim gradient; η_{GI} : learning rate

Output: (x', y') : training data reconstructions

```
1:  $x', y' \leftarrow \mathcal{N}(0, \mathcal{I})$                                 ▷ initialize dummy data
2: while not converged do    ▷ reiterate until some termination criterion is reached
3:    $G' \leftarrow \nabla \mathcal{L}_W(F(x'), y')$                                 ▷ calculate dummy gradient
4:    $GD \leftarrow GDF(G, G')$                                          ▷ calculate gradient distance
5:    $GD \leftarrow GD + \mathcal{R}$                                          ▷ add regularization terms
6:    $x' \leftarrow x' - \eta_{GI} \frac{\partial GD}{\partial x'}; y' \leftarrow y' - \eta_{GI} \frac{\partial GD}{\partial y'}$  ▷ update dummy data
7: return  $(x', y')$ 
```

and reduce the quality of the reconstructions. Improved Deep Leakage from Gradients (iDLG) extends DLG with a deterministic Label Reconstruction Method (LRM) to determine the original client labels y if the softmax function is used for activation of the classification layer and cross-entropy loss as a training objective. Compared to DLG, iDLG only optimizes for x' and sets $y' = y$ by the LRM. The authors found that this improves convergence speed and reconstruction quality (Zhao et al. 2020). The first GI attack that reached a significant milestone in terms of reconstruction quality for large input data with more complex neural networks and larger victim batchsizes is Inverting Gradients (IG) (Geiping et al. 2020). Their proposed attack minimizes the gradient distance in terms of layer-wise cosine distance instead of the Euclidean distance. They use the cosine distance to disentangle the gradient magnitude from its direction. Intuitively this objective aims to find data x' that results in a similar change in the models prediction, i.e., a gradient update G' that follows the same optimization direction as the victim gradient G . Additionally, they apply a regularization scheme based on Total Variation (TV) (Rudin et al. 1992) to increase image fidelity. The authors furthermore found that using the Adam optimizer (Kingma et al. 2014) yields more sophisticated reconstruction results compared to the L-BFGS optimizer. This is especially the case for deeper models and trained models with an overall smaller gradient magnitude. With these simple adjustments to the previous attacks, IG achieves large improvements in terms of reconstruction quality and is the de-facto standard for empirical evaluation of GI attacks and defenses (Hatamizadeh et al. 2022; Gong et al. 2023; Scheliga et al. 2024b).

3.4. Defense Mechanisms

3.4.1. Dropout

Dropout (Hanson 1990; Hinton et al. 2012) is a common regularization technique that randomly masks the output of neurons with a chosen probability p_{dr} . Each forward pass realizes a different version of the model, making Dropout an effective method for model averaging and in turn prevent models from overfitting (Srivastava et al. 2014). Formally, given the output $z^{(l)}$ of the l th layer $\ell^{(l)}$ in a model F , a subsequent Dropout layer $\ell_{dr}^{(l)}$ multiplies $z^{(l)}$ element-wise with a random Dropout mask $\psi^{(l)}$ and scales the remaining outputs according to the Dropout rate p_{dr} to preserve the output magnitude. For every Dropout layer $\ell_{dr}^{(l)}$ $l \in \{1, \dots, L\}$, the Dropout mask $\psi^{(l)}$ is a matrix of independent Bernoulli variables, i.e., $\psi^{(l)} \sim \text{Bernoulli}(p_{dr})$. We denote

$\Psi = \{\psi^{(1)}, \dots, \psi^{(L)}\}$ as the set of L random Dropout masks that are applied during a forward pass through the model F_Ψ .

3.4.2. Differential Privacy

The most common implementation of DP for FL is Differentially Private Stochastic Gradient Descent (DPSGD) (Abadi et al. 2016). During local training, the clients calculate the per-sample gradient g_i for each sample x_i in an input batch with batchsize \mathcal{B} and scale it by division with $\max\left(1, \frac{\|g_i\|_2}{\tau_{\text{clip}}}\right)$. This scaling is applied to ensure that each single input sample does not have too much influence on the overall gradient. The clipping threshold τ_{clip} indicates the maximum gradient norm, that should be allowed for each per-sample gradient. Then, Gaussian noise $\Xi \sim \mathcal{N}(0, \sigma^2 \tau_{\text{clip}}^2 \mathcal{I})$ is added to the accumulated batch gradient. To simplify notation, we denote the execution of these steps as $\tilde{G} = \text{DP}_\Xi(G)$. We use Ξ_C and Ξ_A to refer to the specific noise added by the client and the attacker, respectively.

3.4.3. Gradient Pruning

GP identifies the gradient elements that carry the least training information, i.e., those with the smallest magnitude, and prunes them to zero. For a gradient $G = \{G^{(1)}, \dots, G^{(L)}\}$, Deep Gradient Compression (DGC) (Lin et al. 2017) defines the pruning operation as $\tilde{G} = \text{GP}_\Phi(G) = G \odot \Phi$. Here \odot refers to the layer-wise application of pruning masks Φ . Elements in the pruning masks have the value 0 for gradient elements with the smallest magnitudes and 1, otherwise. The pruning masks are determined for each layers gradient based on a pruning ratio p_{prune} .

3.4.4. Privacy Modules

Recent work proposed to extend models with PMs to protect clients from GI attacks while maintaining high model utility (Scheliga et al. 2022). They implement their PRECODE module as a VB to make feature computation during forwarding stochastic. This in turn, results in stochastic gradients. PRECODE consists of to fully connected layers: an encoder E and a decoder D . During a forward pass in the model, the encoder E encodes a latent feature representation z as $E(z) = [\mu_E, \sigma_E]$. Here $z = I(x)$ represents the latent representations computed by forward propagating an input sample x through all layers of the base model prior to the PRECODE module. Next, a compressed bottleneck representation $\beta_{\text{VB}} \sim \mathcal{N}(\mu_E, \sigma_E)$ is randomly sampled. Since direct sampling from $\mathcal{N}(\mu_E, \sigma_E)$ is a non-differentiable operation with respect to μ_E and σ_E they apply the reparameterization trick described in (Kingma et al. 2013): $\beta_{\text{VB}} = \mu_E + \sigma_E \odot \varepsilon_{\text{VB}}$. Here $\varepsilon_{\text{VB}} \sim \mathcal{N}(0, \mathcal{I})$ is randomly sampled from a standard normal distribution and \odot denotes element-wise multiplication. Finally, the decoder generates a new stochastic representation $D(\beta_{\text{VB}}) = \hat{z}$ which is then used to calculate the model prediction $\hat{y} = O(\hat{z})$. O refers to the layer(s) of the model that follow the VB. The CVB proposed in (Scheliga et al. 2024b) functions in the same way, but only uses convolutional layers instead of fully connected layers. Since convolutional layers make use of parameter-sharing, the number of additional model parameters can be reduced and privacy preserving effects improved.

4. Targeted Attacks – Mimicking Client Behavior

Recent work investigated the privacy preserving effects of Dropout and found that stochastic sampling of the Dropout masks disables the reconstruction of training data through general GI attacks such as IG (Scheliga et al. 2023). Without Dropout, a model F produces deterministic outputs for given inputs. Dropout introduces randomness, making the model F_Ψ stochastic. In each training step new Dropout masks are sampled. This results in different versions of the model, which leads to stochastic predictions and gradients during training. Since an attacker does not have knowledge of the specific Dropout masks Ψ_C that a client C used during training, the attacker applies randomly sampled Dropout masks Ψ_A for the attack. Consequently, the dummy gradients $G' = \nabla \mathcal{L}_W(F_{\Psi_A}(x'), y')$ vary significantly in each attack iteration and will not match the client gradient $G = \nabla \mathcal{L}_W(F_{\Psi_C}(x), y)$. As a result, the attacker is unable to compute sufficient reconstructions (Scheliga et al. 2023). In response they propose a Dropout Inversion Attack (DIA) that approximates $F_{\Psi_A} \approx F_{\Psi_C}$ by joint optimization of Ψ_A during the GI attack. If a sufficient approximation is found, the attack can mimic the gradient computation process of the client and therefore bypass the protection of Dropout. In the following section we adopt this attack principle and show how it can be applied to other defense mechanisms. In particular, we will empirically demonstrate, that if an attacker can sufficiently approximate and mimic the gradient computation process of the client, the protection of DP, GP, PRECODE and CVB can be bypassed.

Throughout the following sections we show experimental results for some preliminary experiments to provide an empirical proof of concept for the performance of the described attacks. We compare the IG attack with our proposed targeted attack variations for a Convolutional Neural Network (CNN) and Vision Transformer (ViT) on the MNIST (LeCun et al. 1998) and CIFAR-10 (Krizhevsky et al. 2009) datasets. We measure reconstruction quality in terms of Structural Similarity (SSIM) and Attack Success Rate (ASR). Details on the experimental setup for all reconstruction experiments in this paper are presented in Section 5.

4.1. Differential Privacy Inversion Attack

Unlike Dropout, DP does not create different model realizations, as both the client and attacker use the same deterministic model F for gradient computation. Instead, DP adds randomness directly to the training gradients, causing different realizations of the exchanged gradients. An attacker aims to find dummy images x' so that the dummy gradients closely match the client’s original training gradients, i.e., $G' = G$. However, the client sends the perturbed gradients \tilde{G} to the server. Therefore, the attacker must optimize the distance between the dummy gradients G' and the perturbed client gradients \tilde{G} . Since $\tilde{G} = \text{DP}_{\Xi_C}(G)$ is inherently different compared to G , reconstruction quality decreases with larger differences between \tilde{G} and G .

While DP can protect from GI attacks when sufficient noise is added, previous studies show that low levels of noise are insufficient to prevent data reconstruction (Huang et al. 2021; Scheliga et al. 2024b). However, we argue, that even with high noise levels, if the attacker has access to the specific noise Ξ_C added by the client, they could still reconstruct the training data. This is because the attacker could fully mimic the gradient computation process, using $\text{GDF}(\tilde{G}, \tilde{G}')$ for optimization, where $\tilde{G} = \text{DP}_{\Xi_C}(G)$ and $\tilde{G}' = \text{DP}_{\Xi_C}(G')$. We test this assumption in by giving the attacker access to

the client’s noise, i.e., $DP_{\Xi_A} = DP_{\Xi_C}$. Consistent with the *well-informed attack* on Dropout in (Scheliga et al. 2023), we refer to this attack as Well-Informed Inverting Gradients (WIIG). Based on a set of preliminary experiments, we apply DP with parameters $\tau_{\text{clip}} = 20$ and $\sigma = 10^{-3}$. This level of noise noticeably impacted the reconstruction quality of the IG attack while minimizing the impact on model utility.

Table 1. Privacy metrics for IG, WIIG and DPIA for training gradients defended with DP. The training gradients are attacked for the CNN and ViT on the MNIST and CIFAR-10 datasets. Arrows indicate direction of improvement from the viewpoint of a defending client. Bold and italic formatting highlight best and worst results, respectively.

		Model	DP ($\tau_{\text{clip}}, \sigma$)	Attack	SSIM \downarrow	ASR [%] \downarrow
MNIST	CNN	-	-	IG	<i>0.95 (± 0.06)</i>	100
				IG	0.64 (± 0.11)	85.16
		(20, 10^{-3})	(20, 10^{-3})	WIIG	<i>0.90 (± 0.06)</i>	100
				DPIA	0.29 (± 0.13)	5.47
	ViT	-	-	IG	<i>0.99 (± 0.00)</i>	100
				IG	0.55 (± 0.09)	76.56
		(20, 10^{-3})	(20, 10^{-3})	WIIG	<i>0.94 (± 0.03)</i>	100
				DPIA	0.08 (± 0.06)	0
CIFAR-10	CNN	-	-	IG	<i>0.87 (± 0.11)</i>	96.88
				IG	0.31 (± 0.11)	5.47
		(20, 10^{-3})	(20, 10^{-3})	WIIG	<i>0.82 (± 0.06)</i>	100
				DPIA	0.26 (± 0.10)	1.56
	ViT	-	-	IG	<i>0.90 (± 0.05)</i>	100
				IG	0.21 (± 0.07)	0
		(20, 10^{-3})	(20, 10^{-3})	WIIG	<i>0.77 (± 0.08)</i>	100
				DPIA	0.09 (± 0.04)	0

Table 1 shows the results of these experiments. Compared to an unprotected baseline model, DP reduces the reconstruction quality under the IG attack. For the CNN, IG achieves an ASR of 85.16% on MNIST and 5.47% on CIFAR-10. For the ViT, the ASR is 76.56% and 0%, respectively. As expected, WIIG increases the ASR to 100% across all models and datasets, as it replicates the exact gradient computation process performed by the client during local training. Therefore, if an attacker can sufficiently approximate the noise and scaling factor, reconstruction quality should improve compared to a baseline IG attack.

In reality, the attacker does not have access to DP_{Ξ_C} . However, similar to the Dropout mask approximations in DIA (Scheliga et al. 2023), the attacker can attempt to approximate the client’s noise, aiming for $DP_{\Xi_A} \approx DP_{\Xi_C}$, i.e., $\Xi_A \approx \Xi_C$. We implement this approach as a DPIA. In addition to the general GI attack, the attacker randomly initializes dummy noise $\Xi_A = \{\xi_A^{(l)} \sim \mathcal{N}(0, \sigma^2 \tau_{\text{clip}}^2 \mathcal{I}) | \forall l = 1, \dots, L\}$. During the attack, this dummy noise is applied to the dummy gradients, i.e., $\tilde{G}' = DP_{\Xi_A}(G')$, and the gradient distance is calculated between the perturbed client gradient G and the dummy perturbed gradients \tilde{G}' . In each attack iteration, the attacker adjusts the dummy noise based on the gradient distance with respect to the dummy noise. Additionally, we regularize the dummy noise to have a mean of 0 and a standard deviation of $\sigma^2 \tau_{\text{clip}}^2$. If the attacker can sufficiently approximate the noise such that

$\Xi_A \approx \Xi_C$, we expect the reconstruction quality of the dummy data to improve.

However, the results in Table 1 indicate that DPIA does not find sufficient approximations Ξ_A . In fact, the reconstruction quality using DPIA is significantly lower than with IG, as indicated by the reduced SSIM values and an ASR close to or equal to 0%. While DPIA computes dummy gradients \tilde{G}' that closely match the victim’s perturbed gradients \tilde{G} , this does not translate to high-quality reconstructions. Since DPIA jointly optimizes the dummy noise and the dummy data by minimizing the GDF, there are too many possibilities for the dummy noise to compensate for misalignments between the victim’s and dummy’s gradients. In the worst case, DPIA may only be optimizing for an optimal dummy noise to minimize the gradient distance, while the dummy data remains of poor quality. Although we were unable to sufficiently approximate the noise applied by the client using DP, and thus did not improve reconstruction quality, it is important to note that DP always involves a trade-off between model utility and privacy. While WIIG achieves an ASR of 100%, this was only considered as a proof of concept. In a realistic scenario, an attacker would not have access to the ground truth noise applied by the client.

4.2. Gradient Pruning Inversion Attack

Unlike Dropout, DP, PRECODE, and CVB, GP does not affect gradient computation through stochastic processes. Instead, it deterministically prunes gradient values based on their magnitude. Intuitively the main defensive capability of GP against GI attacks is the reduced amount of gradient information available for attack optimization. However, since only the lowest magnitude values are typically pruned, information on the most important feature activations in the model is still retained. This suggests that even with high pruning rates, this information could be sufficient for GI attacks. We argue that the primary reason for the decrease in reconstruction quality when GP is applied is that the attacker does not mimic the pruning step used by the client during gradient computation. Without applying a similar pruning regimen, it becomes challenging, if not impossible, for the attacker to find dummy data x' that results in a dummy gradient G' that is as sparse as the pruned client gradient $\tilde{G} = \text{GP}_{\Phi_C}(G)$. Fortunately for the attacker, the client reveals the pruning masks used during local training. The ground truth pruning masks $\Phi_C = \{\phi_C^{(1)}, \dots, \phi_C^{(L)}\}$ can be determined as follows:

$$\phi_C^{(l)} = \mathbf{1} \left(\text{abs} \left(G^{(l)} \right) > 0 \right) \forall l = 1, \dots, L. \quad (2)$$

Here, $\mathbf{1}$ denotes that elements in $\phi_C^{(l)}$ are set to 1 if the corresponding gradient elements meet the condition and are set to 0 otherwise. We implement a GPIA that takes advantage of this knowledge by applying the client’s pruning mask Φ_C to the dummy gradients G' during the attack optimization, i.e., $\tilde{G}' = \text{GP}_{\Phi_C}(G')$. As a result, the zero values in \tilde{G} and \tilde{G}' match by default. Previous studies indicate that high pruning rates p_{prune} are required to have any significant impact on privacy preservation (Scheliga et al. 2024b). This means that typically at least 90% of the values in \tilde{G} and \tilde{G}' match by default. Since \tilde{G} retains the most informative gradient values, i.e., those with the highest magnitude, these might be sufficient to reconstruct the client’s training data x from the dummy data x' .

We evaluate the performance of GPIA on GP-protected gradients and compare it to the IG attack. We do not explicitly consider a WIIG attacker, as GPIA computes

Table 2. Privacy metrics for IG and GPIA for training gradients defended with GP with increasing pruning rates p_{prune} . The training gradients are attacked for the CNN and ViT on the MNIST and CIFAR-10 datasets. Arrows indicate direction of improvement from the viewpoint of a defending client. Bold and italic formatting highlight best and worst results, respectively.

	Model	GP p_{prune}	Attack	SSIM \downarrow	ASR [%] \downarrow
MNIST	CNN	-	IG	<i>0.95 (± 0.06)</i>	100
			IG	0.63 (± 0.09)	89.84
		0.90	GPIA	0.91 (± 0.07)	100
		0.95	IG	0.52 (± 0.08)	64.06
			GPIA	0.82 (± 0.12)	99.22
	ViT	0.99	IG	0.24 (± 0.05)	0
			GPIA	0.50 (± 0.13)	49.22
		-	IG	<i>0.99 (± 0.00)</i>	100
			IG	0.20 (± 0.06)	0
CIFAR-10	CNN	0.90	IG	0.48 (± 0.08)	46.88
			GPIA	0.70 (± 0.12)	90.62
		0.95	IG	0.32 (± 0.07)	0
			GPIA	0.53 (± 0.15)	66.41
	ViT	0.99	IG	0.15 (± 0.04)	0
			GPIA	0.29 (± 0.13)	3.91
		-	IG	<i>0.90 (± 0.05)</i>	100
			IG	0.09 (± 0.04)	0
		0.90	GPIA	0.77 (± 0.07)	100
		0.95	IG	0.02 (± 0.02)	0
			GPIA	0.71 (± 0.08)	100
		0.99	IG	0.01 (± 0.01)	0
			GPIA	0.59 (± 0.09)	83.59

the ground truth pruning masks, which are inherently part of the exchanged training gradients. We test both attacks for increasing pruning ratios $p_{\text{prune}} \in \{0.90, 0.95, 0.99\}$ to determine the level of gradient sparsity required to effectively prevent the reconstruction of training data. The results of these experiments are shown in Table 2. For both datasets, models, and all considered pruning rates p_{prune} , GPIA consistently improves reconstruction quality compared to IG, as indicated by higher SSIM and ASR. As expected, since only the gradients with the smallest magnitudes are pruned, enough information for reconstruction often remains. By mimicking the full gradient computation process, including the application of GP, rather than just gradient computation as in IG, the GPIA attacker can better optimize the dummy data to match the victim’s gradients. However, as the pruning rate increases, ASR decreases for the CNN. For a pruning rate of $p_{\text{prune}} = 0.95$, GPIA achieves an ASR of 99.22% and

66.41% for MNIST and CIFAR-10, respectively, while a pruning rate of $p_{\text{prune}} = 0.99$ results in ASR values of 49.22% and 3.91% for the same datasets. For the ViT, this decrease in reconstruction quality requires higher pruning rates and more complex data. For MNIST, GPIA achieves an ASR of 100% for all pruning rates, compared to 0% under IG. For CIFAR-10, the ASR can be reduced to 83.59% with a pruning rate of $p_{\text{prune}} = 0.99$. We suspect that for the ViT, reconstruction quality is less affected because the overall number of parameters is significantly larger compared to our considered CNN. For example, with a large pruning rate of $p_{\text{prune}} = 0.99$, 660 and 16,092 non-zero gradient values remain for attack optimization for the CNN and ViT, respectively. Depending on the size of the model, even at high pruning rates there is still enough gradient information left to achieve good reconstructions.

4.3. Variational Bottleneck Inversion Attack

Similar to Dropout the defensive capabilities of the VB-based PMs PRECODE and CVB come from the randomness induced by the stochastic sampling during the forwarding step. They turn the deterministic model F into a stochastic one, that depends on the sampled values of ε_{VB} , which are required for the reparameterization trick during model training. Since ε_{VB} is randomly sampled in each optimization step, small changes in the dummy image x' lead to an increased entropy of the dummy’s latent representations $D(\beta_{\text{VB}}) = \hat{z}$. This makes it difficult for the optimizer to find dummy images x' that minimize the reconstruction loss.

Hence, to sufficiently mimic the client gradient computation process, an attacker has to approximate the randomly sampled reparameterization matrix $\varepsilon_{\text{VB}_C}$. We implement VBIA accordingly, by jointly optimizing for $\varepsilon_{\text{VB}_C}$ during the attack optimization process. In addition to the general GI attack, the attacker randomly initializes a dummy reparameterization matrix $\varepsilon_{\text{VB}_A} \sim \mathcal{N}(0, \mathcal{I})$. During forward passes in the attack optimization process, this dummy reparameterization matrix is used instead of a randomly sampled one in the VB. In each attack iteration, the attacker updates both the dummy data and the dummy reparameterization matrix $\varepsilon_{\text{VB}_A}$ based on the gradient distance GD. If the attacker can sufficiently approximate the reparameterization matrix such that $\varepsilon_{\text{VB}_A} \approx \varepsilon_{\text{VB}_C}$, the reconstruction quality of the dummy data is expected to improve.

We evaluate the performance of VBIA on PRECODE and CVB protected gradients and compare it to the Partial Inverting Gradients (PIG) ("Ignore attack") proposed in (Scheliga et al. 2024b). By excluding the most stochastic gradients from gradient distance calculation during attack optimization, PIG was shown to achieve better reconstructions for PRECODE and CVB compared to IG. For comparison, we evaluate a WIIG attack, where the attacker has access to the true reparameterization matrix $\varepsilon_{\text{VB}_C}$ sampled by the client during training, i.e., $\varepsilon_{\text{VB}_A} = \varepsilon_{\text{VB}_C}$. In reality, however, the attacker does not have this knowledge and must approximate $\varepsilon_{\text{VB}_A} \approx \varepsilon_{\text{VB}_C}$. We parameterize PRECODE and CVB as recommended in (Scheliga et al. 2024b).

The results of these experiments can be found in Table 3. Although both PMs provide protection against the PIG attack, their privacy preserving effect is significantly reduced when attacked with VBIA. If the attacker has knowledge of the reparameterization matrix that was stochastically sampled during the client’s training process as in the WIIG attack, data can be reconstructed with high quality because the attacker uses the same model realization as the client, i.e., $\varepsilon_{\text{VB}_A} = \varepsilon_{\text{VB}_C}$. However, even without this knowledge, the experiments show that the VBIA attacker can sufficiently approx-

imate the reparameterization matrix $\varepsilon_{VB_A} \approx \varepsilon_{VB_C}$. For the CNN, the ASR increases from less than 8% with PIG to over 93% with VBIA for both datasets and PMs. For the ViT, the VBIA achieves an ASR of 100% in all cases.

4.4. Combined Defenses Inversion Attack

The previous sections discussed GI attacks to bypass the defensive mechanisms of Dropout (DIA (Scheliga et al. 2023)), GP (GPIA), PRECODE, and CVB (VBIA). We observed that if an attacker is able sufficiently approximate and mimic the client’s gradient computation process, single defenses can be bypassed. We therefore propose to combine multiple defense mechanisms. This increases the complexity of the attack, as the attacker must approximate multiple sources of stochasticity to sufficiently mimic

Table 3. Privacy metrics for PIG, WIIG and VBIA. The models use either PRECODE or a CVB as privacy module. The training gradients are attacked for the CNN and ViT on the MNIST and CIFAR-10 datasets. Arrows indicate direction of improvement from the viewpoint of a defending client. Bold and italic formatting highlight best and worst results, respectively.

	Model	Defense	Attack	SSIM ↓	ASR [%] ↓
MNIST	CNN	-	IG	<i>0.95 (±0.06)</i>	<i>100</i>
			PIG	0.42 (±0.09)	21.09
		PRECODE	WIIG	<i>0.87 (±0.13)</i>	<i>98.44</i>
		VBIA	<i>0.95 (±0.07)</i>	<i>100</i>	
	CVB	PIG	0.29 (±0.09)	0.78	
			<i>0.95 (±0.04)</i>	<i>100</i>	
		VBIA	<i>0.88 (±0.09)</i>	<i>99.22</i>	
	ViT	-	IG	<i>0.99 (±0.00)</i>	<i>100</i>
			PIG	0.04 (±0.02)	0
		PRECODE	WIIG	<i>0.99 (±0.00)</i>	<i>100</i>
		VBIA	<i>0.94 (±0.03)</i>	<i>100</i>	
		CVB	PIG	<i>0.37 (±0.08)</i>	<i>7.03</i>
			WIIG	<i>1.00 (±0.00)</i>	<i>100</i>
			VBIA	<i>1.00 (±0.00)</i>	<i>100</i>
CIFAR-10	CNN	-	IG	<i>0.87 (±0.11)</i>	<i>96.88</i>
			PIG	0.32 (±0.09)	3.91
		PRECODE	WIIG	<i>0.83 (±0.15)</i>	<i>96.09</i>
		VBIA	<i>0.88 (±0.07)</i>	<i>99.22</i>	
		CVB	PIG	0.21 (±0.08)	0
			WIIG	<i>0.78 (±0.14)</i>	<i>92.19</i>
			VBIA	<i>0.72 (±0.13)</i>	<i>93.75</i>
	ViT	-	IG	<i>0.90 (±0.05)</i>	<i>100</i>
			PIG	0.03 (±0.02)	0
		PRECODE	WIIG	<i>0.93 (±0.03)</i>	<i>100</i>
		VBIA	<i>0.81 (±0.07)</i>	<i>100</i>	
		CVB	PIG	<i>0.16 (±0.06)</i>	0
			WIIG	<i>1.00 (±0.00)</i>	<i>100</i>
			VBIA	<i>1.00 (±0.00)</i>	<i>100</i>

Algorithm 2 Combined Defenses Inversion Attack (CDIA)

Input: F : neural network; \mathcal{L} : training loss function; GDF: gradient distance function; $\tilde{G} = \text{GP}_{\Phi_C}(\text{DP}_{\Xi_C}(\nabla \mathcal{L}_W(F_{(\Psi_C, \varepsilon_{\text{VB}_A})(x)}, y)))$: perturbed and pruned victim gradient; η_{GI} : learning rate; p_{dr} : Dropout rate;

Output: (x', y') training data reconstructions;

$\Psi_A = \{\psi_A^{(1)}, \dots, \psi_A^{(L)}\}$: approximated Dropout masks;

Φ_C : client pruning mask;

$\varepsilon_{\text{VB}_A}$: approximated reparameterization matrix

```

1:  $x', y' \leftarrow \mathcal{N}(0, \mathcal{I})$                                       $\triangleright$  initialize dummy data
2: if Client used Dropout then
3:    $\psi_A^{(1)}, \dots, \psi_A^{(L)} \leftarrow \text{Bernoulli}(p_{\text{dr}})$             $\triangleright$  initialize dummy Dropout masks
4: if Client used GP then
5:    $\Phi_C \leftarrow \text{abs}(\tilde{G}) > 0$                                       $\triangleright$  compute client pruning mask
6: if Client used PRECODE/CVB then
7:    $\varepsilon_{\text{VB}_A} \leftarrow \mathcal{N}(0, \mathcal{I})$                                 $\triangleright$  initialize dummy reparameterization matrix
8: while not converged do    $\triangleright$  reiterate until some termination criterion is reached
9:    $G' \leftarrow \nabla \mathcal{L}_W(F_{(\Psi_A, \varepsilon_{\text{VB}_A})(x')}, y')$             $\triangleright$  calculate dummy gradient
10:  if Client used GP then
11:     $\tilde{G}' \leftarrow G' \odot \Phi_C$                                           $\triangleright$  apply pruning mask
12:     $\text{GD} \leftarrow \text{GDF}(\tilde{G}, \tilde{G}')$                           $\triangleright$  calculate gradient distance
13:     $\text{GD} \leftarrow \text{GD} + \mathcal{R}$                                       $\triangleright$  add regularization terms
14:     $x' \leftarrow x' - \eta_{\text{GI}} \frac{\partial \text{GD}}{\partial x'}; y' \leftarrow y' - \eta_{\text{GI}} \frac{\partial \text{GD}}{\partial y'}$             $\triangleright$  update dummy data
15:  if Client used Dropout then
16:     $\psi_A^{(l)} \leftarrow \psi_A^{(l)} - \eta_{\text{GI}} \frac{\partial \text{GD}}{\partial \psi_A^{(l)}} \forall l \in 1, \dots, L$             $\triangleright$  update dummy Dropout masks
17:  if Client used PRECODE/CVB then
18:     $\varepsilon_{\text{VB}_A} \leftarrow \varepsilon_{\text{VB}_A} - \eta_{\text{GI}} \frac{\partial \text{GD}}{\partial \varepsilon_{\text{VB}_A}}$             $\triangleright$  update dummy reparameterization matrix
19: return  $(x', y'), \Psi_A, \Phi_C, \varepsilon_{\text{VB}_A}$ 

```

the client’s gradient computation process. This could lead to an unstable attack optimization process, which in turn would result in reduced reconstruction quality and higher privacy. To find an optimal combination of defenses, we conduct an extensive ablation study that tests various combinations.

To rigorously test the defensive capabilities of these defense combinations, we formulate a Combined Defenses Inversion Attack (CDIA). CDIA combines the above attacks by targeting all applied defenses during the attack optimization process if the client used them during local training. Since DP decreased reconstruction quality compared to IG, we do not specifically target DP in CDIA. For CDIA, we assume that the attacker has knowledge of the defense mechanisms employed by the client. This assumption is coherent with the threat model discussed in Section 3.2. Dropout, PRECODE, and CVB are integrated into the model architecture and are known to the server, as it coordinates the federated training process. Even if the attacker does not directly possess this information, it could be inferred from the shapes of the transmitted gradients. While DP might be more challenging to detect, CDIA does not specifically target this defense. The use of GP, however, can be easily inferred from the sparsity of the transmitted gradients.

A detailed description of CDIA is provided in Algorithm 2. The attack adapts based on the defenses used by the client. If Dropout was applied, CDIA includes Dropout mask approximation in the joint optimization process. If GP was used, the attacker calculates the ground truth pruning masks and applies them to the dummy gradient before calculating the gradient distance GD. For PRECODE and CVB, the attacker approximates the reparameterization matrix during optimization. For further details on each of the targeted attack mechanisms, please refer to the respective sections above. Note, that when no defense is applied, CDIA defaults to the basic IG attack. When a single defense mechanism is used, CDIA corresponds to DIA for Dropout, IG for DP, GPIA for GP, and VBIA for PRECODE and CVB.

5. Experimental Setup

This section describes the general settings for the experiments in this paper. For most experiments we used the same simple CNN model as in (Scheliga et al. 2024b). It consists of three convolutional layers with 5×5 kernels, [16, 32, 64] channels, a stride of 2 and ReLU activation. The last layer of the CNN is a fully connected classification layer with 10 neurons and softmax activation. The following sections describe more details on how we measured model utility and privacy leakage.

5.1. Model Utility

We train models for image classification on the MNIST (LeCun et al. 1998) and CIFAR-10 (Krizhevsky et al. 2009) datasets. The datasets are first separated into training and test splits according to the corresponding benchmark protocols. We embedded all experiments in a FL scenario with 10 clients. The training data splits are independent and identically distributed to those 10 clients. Each client creates a validation split that corresponds to 10% of the training data. This leaves every client with 5'400/4'500 training samples, 600/400 validation samples, and 1'000/1'000 test samples for MNIST/CIFAR-10 respectively.

The clients collaboratively train a randomly initialized model for 300 communication rounds with one local training epoch using FedAvg (McMahan et al. 2017a). Local training minimizes the cross-entropy loss using Adam optimizer (Kingma et al. 2014) with a learning rate of 0.001, momentum parameters of $(\beta_1, \beta_2) = (0.9, 0.999)$, and a batch size of 64. To save computational resources, we stop the training early, if the mean validation loss over all clients has not improved for 40 consecutive communication rounds. To measure model utility, we calculate the accuracy of the global model states on the test data after every communication round. We repeated each experiment and report the mean and standard deviation across three runs with different random seeds.

5.2. Privacy

For each of the datasets we create a victim dataset to evaluate privacy leakage. The victim dataset is composed of 128 images that are randomly sampled from the training data of one client.

We aim to empirically identify an upper bound for privacy leakage via iterative GI attacks and test the limits of the investigated defense mechanisms. To this end, we consider the *worst-case defense scenario* for an attacked client. Unless not otherwise

stated, we use a batch size $\mathcal{B} = 1$ and only perform a single local training step before transmitting the victim gradient to the attacker. As discussed in Section 2.2, previous work has shown that higher batch size and multiple local training iterations increase the difficulty of the attack, thereby decreasing privacy leakage. If the defense mechanism works even in such *hard to defend* settings, privacy leakage becomes even more improbable in realistic training scenarios (Wei et al. 2020; Huang et al. 2021).

We use our proposed CDIA attack to target and bypass each of applied defenses. We configure it so that it defaults to a baseline IG attack (Geiping et al. 2020) if no defenses or only DP is applied. In detail, dummy images are initialized from a Gaussian distribution, cosine distance is used as loss function, and TV as regularization term with weight $\lambda_{\text{TV}} = 0.01$. We use Adam optimizer with initial learning rate 1 and reduce it by a factor of 0.1 if the reconstruction loss plateaus for 400 attack iterations. To save computational resources, attacks are stopped if either the reconstruction loss falls below a value of 10^{-5} , or there is no decrease in reconstruction loss for 4'000 iterations, or after a maximum of 20,000 iterations. Furthermore, we assume that the label information for each reconstruction is known, as it can be analytically reconstructed from gradients of cross-entropy loss functions with respect to the weights of fully connected layers with softmax activation (Geiping et al. 2020; Zhao et al. 2020; Wei et al. 2020). We ensured that our threat model (cf. Section 3.2) and the described attack simulation setup is consistent with related work (Zhu et al. 2019; Geiping et al. 2020; Wei et al. 2020; Scheliga et al. 2023; Scheliga et al. 2024b).

For each reconstructed image, we calculate the reconstruction quality by comparing it with the original image from the victim dataset. While Mean Squared Error (MSE) and Peak Signal to Noise Ratio (PSNR) are commonly used metrics for assessing reconstruction quality, they often do not correlate well with human visual perception (Wang et al. 2004). Therefore, we use SSIM (Wang et al. 2004) as the primary metric for measuring reconstruction quality. Since we report the average SSIM value over all reconstructions, extremely good or bad reconstructions might be missed. Therefore, we additionally compute the ASR as the fraction of the successfully reconstructed images of the victim dataset (Wagner et al. 2018). We consider an image to be successfully reconstructed if the SSIM value is above a threshold of $\tau_{\text{ASR}} = 0.5$.

5.3. Ablation Study of Defense Mechanisms

We conduct an extensive ablation study, to examine all possible combinations of the previously discussed defense mechanisms, including Dropout, DP, GP, and one of the PMs (either PRECODE or CVB). For Dropout, we apply a modest Dropout rate of $p_{\text{dr}} = 0.25$, as previous studies showed a decrease of model utility for higher rates (Scheliga et al. 2023). When using perturbation-based defenses, we maintain low levels of perturbation to preserve an acceptable trade-off between model utility and privacy. Specifically, we use a clipping threshold of $\tau_{\text{clip}} = 20$ and a noise multiplier $\sigma = 10^{-4}$ for DP, and a pruning rate of $p_{\text{prune}} = 0.50$ for GP. Previous studies indicate that higher perturbation rates have a significant negative impact on model utility (Scheliga et al. 2024b). For PRECODE and CVB we apply the hyperparameter configurations recommended in (Scheliga et al. 2024b).

6. Experimental Results & Discussion

6.1. Ablation Study

First, we conducted an extensive ablation study that investigates the impact on model utility and privacy of all potential defense combinations of the investigated defenses. The results for these experiments can be found in Table 4. Example reconstructions are displayed in Figure 2. For the MNIST dataset, model utility did not vary significantly across the defense combinations. The baseline model without any defense achieved an accuracy of 99.10%. Models utilizing a CVB generally performed slightly better, with the highest accuracy of 99.19% achieved by the DP+GP+CVB combination. However, most other defense combinations slightly reduced model utility, with the lowest accuracy of 98.19% resulting from the DP+PRECODE combination. When attacked by CDIA, single defenses and most defense combinations were unable to protect the privacy of the training data, as indicated by an ASR close to 100%. Without a PM, the lowest ASR achieved was around 70% for DO+DP and DO+DP+GP. However, defense combinations involving PRECODE reduced ASR to between 27.34% and 54.69% for DO+DP+GP+PRECODE and DP+GP+PRECODE, respectively. While these combinations improved privacy to some extent, they also reduced model utility compared to the baseline. Only defense combinations utilizing both DP and CVB reduced ASR to 0%. The gradient scaling and slight noise introduced by DP appears sufficient to disrupt CDIA, specifically hindering the optimization of ε_{VBA} and destabilizing the attack optimization. For MNIST, the best combination in terms of both model utility and privacy was DP+GP+CVB, resulting in an ASR of 0% and an accuracy of 99.19%.

For the CIFAR-10 dataset, both accuracy and reconstruction quality were consistently lower due to the higher complexity of the dataset. However, the general trends for the defense combinations remained similar. Defense combinations involving CVB noticeably improved accuracy compared to the unprotected baseline model, with the highest accuracy of 67.80% achieved by the DO+CVB combination, representing an improvement of 5.27%. Introducing PRECODE harmed model utility more significantly on CIFAR-10, with the worst case being DP+GP+PRECODE, where accuracy dropped by 6.27% compared to the baseline model. Again, single defenses and most defense combinations were ineffective at protecting privacy, with ASR remaining close to 100%. Combinations involving DO+DP, DP+PRECODE, and DP+CVB were the only ones that significantly reduced ASR to below 20%. Notably, only the combinations of DP and CVB consistently reduced ASR to 0%, highlighting the importance of this combination for privacy protection against CDIA.

While DO and GP are not strictly required for privacy preservation, they can enhance model utility due to their regularizing effects, provided they are applied with moderate Dropout and pruning rates. For CIFAR-10, the best combination in terms of both model utility and privacy was DO+DP+CVB, which resulted in an ASR of 0% and an accuracy of 66%, boosting model utility by 3.47% compared to the unprotected baseline model.

6.2. Application to other Model Architectures

Next, we investigate the trade-off between model utility and privacy when applying various defense mechanism combinations to different model architectures. Specifically, we consider a ResNet-18 (He et al. 2016) and a small ViT (Dosovitskiy et al. 2020)

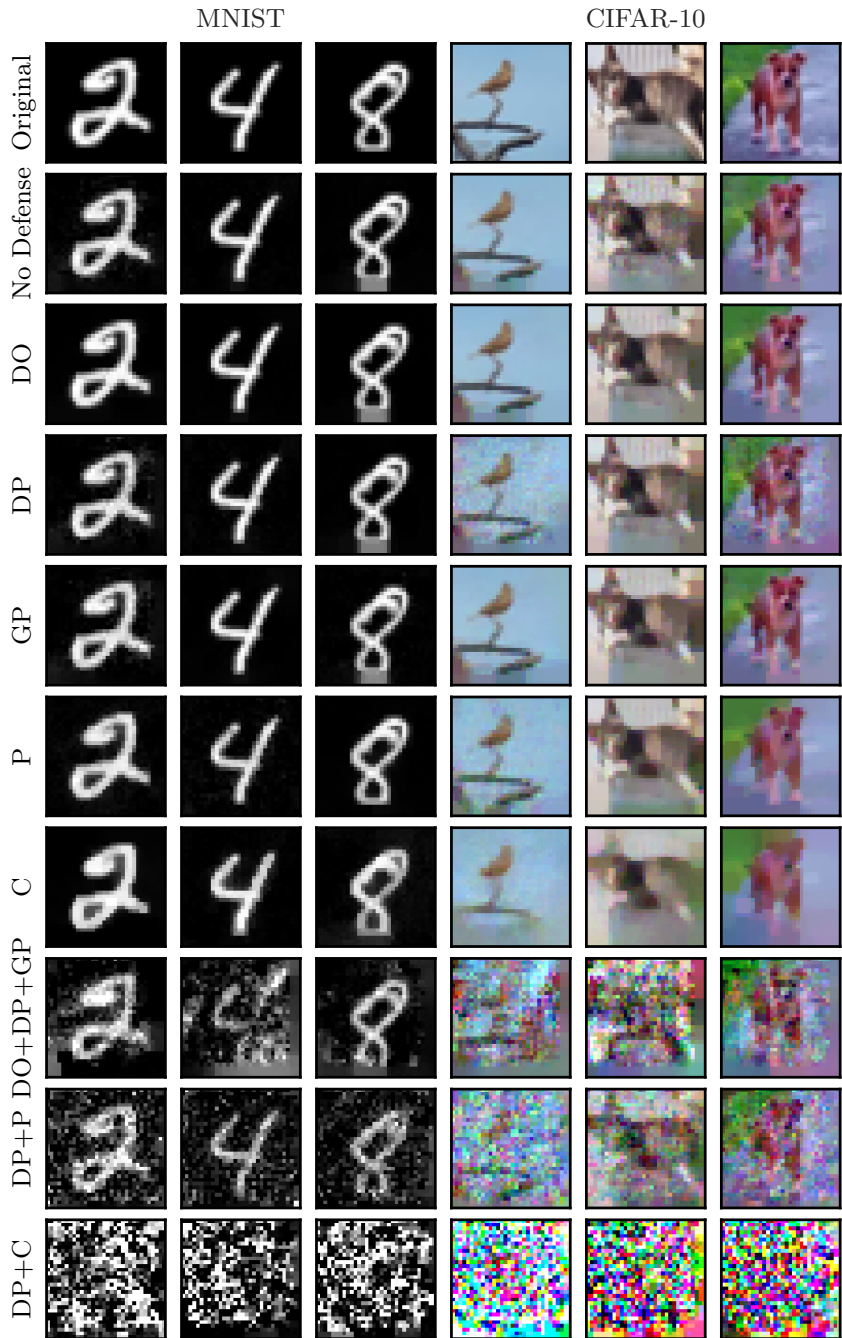


Figure 2. Example reconstructions for the CNN on the MNIST and CIFAR-10 datasets when protected with different defense combinations. We illustrate examples for Dropout (DO), DP, GP, PRECODE (P) and CVB (C).

Table 4. Model utility and privacy metrics for an ablation study using different combinations of defense mechanisms in the CNN on the MNIST and CIFAR-10 dataset. We consider Dropout (DO), Differential Privacy (DP), Gradient Pruning (GP) and a Privacy Module (PM) as defense. ✓ and ✗ indicate, whether a defense mechanism was used or not. P and C indicate whether PRECODE or CVB was used, respectively. Arrows indicate direction of improvement from the viewpoint of a defending client. Bold and italic formatting highlight best and worst results, respectively.

	DO	DP	GP	PM	SSIM ↓	ASR [%] ↓	Accuracy [%] ↑
MNIST	✗	✗	✗	✗	0.95 (± 0.06)	100	99.10 (± 0.04)
	✗	✗	✗	P	0.95 (± 0.07)	100	98.33 (± 0.02)
	✗	✗	✗	C	0.88 (± 0.09)	99.22	99.15 (± 0.05)
	✗	✗	✓	✗	0.95 (± 0.04)	100	99.00 (± 0.09)
	✗	✗	✓	P	0.93 (± 0.09)	100	98.41 (± 0.04)
	✗	✗	✓	C	0.84 (± 0.08)	99.22	99.06 (± 0.05)
	✗	✓	✗	✗	0.93 (± 0.06)	100	99.06 (± 0.00)
	✗	✓	✗	P	0.49 (± 0.12)	50.78	98.19 (± 0.03)
	✗	✓	✗	C	0.14 (± 0.05)	0	99.18 (± 0.00)
	✗	✓	✓	✗	0.95 (± 0.05)	100	98.97 (± 0.05)
	✗	✓	✓	P	0.50 (± 0.13)	54.69	98.22 (± 0.14)
	✗	✓	✓	C	0.14 (± 0.04)	0	99.19 (± 0.05)
	✓	✗	✗	✗	0.97 (± 0.02)	100	99.12 (± 0.03)
	✓	✗	✗	P	0.97 (± 0.04)	100	98.41 (± 0.02)
	✓	✗	✗	C	0.91 (± 0.06)	100	99.09 (± 0.08)
	✓	✗	✓	✗	0.97 (± 0.02)	100	98.95 (± 0.06)
	✓	✗	✓	P	0.96 (± 0.06)	100	98.24 (± 0.03)
	✓	✗	✓	C	0.85 (± 0.09)	99.22	99.05 (± 0.03)
	✓	✓	✗	✗	0.56 (± 0.14)	69.53	99.06 (± 0.05)
	✓	✓	✗	P	0.40 (± 0.20)	39.06	98.28 (± 0.00)
	✓	✓	✗	C	0.12 (± 0.06)	0	99.12 (± 0.01)
	✓	✓	✓	✗	0.56 (± 0.14)	71.88	98.95 (± 0.04)
	✓	✓	✓	P	0.37 (± 0.19)	27.34	98.23 (± 0.03)
	✓	✓	✓	C	0.12 (± 0.05)	0	99.15 (± 0.06)
CIFAR-10	✗	✗	✗	✗	0.87 (± 0.11)	96.88	62.53 (± 0.16)
	✗	✗	✗	P	0.88 (± 0.07)	99.22	59.48 (± 0.23)
	✗	✗	✗	C	0.72 (± 0.13)	93.75	67.19 (± 0.64)
	✗	✗	✓	✗	0.86 (± 0.09)	98.44	62.53 (± 0.34)
	✗	✗	✓	P	0.86 (± 0.10)	98.44	59.53 (± 0.11)
	✗	✗	✓	C	0.66 (± 0.09)	92.97	67.34 (± 0.28)
	✗	✓	✗	✗	0.83 (± 0.11)	97.66	62.31 (± 0.00)
	✗	✓	✗	P	0.40 (± 0.14)	25.78	57.39 (± 0.26)
	✗	✓	✗	C	0.04 (± 0.02)	0	65.86 (± 0.25)
	✗	✓	✓	✗	0.81 (± 0.10)	96.88	60.72 (± 0.51)
	✗	✓	✓	P	0.35 (± 0.14)	16.41	56.26 (± 0.01)
	✗	✓	✓	C	0.04 (± 0.02)	0	65.45 (± 1.04)
	✓	✗	✗	✗	0.91 (± 0.05)	100	64.36 (± 0.12)
	✓	✗	✗	P	0.89 (± 0.07)	99.22	59.77 (± 0.16)
	✓	✗	✗	C	0.75 (± 0.08)	100	67.80 (± 0.41)
	✓	✗	✓	✗	0.88 (± 0.05)	100	62.43 (± 0.24)
	✓	✗	✓	P	0.87 (± 0.07)	100	59.83 (± 0.34)
	✓	✗	✓	C	0.67 (± 0.11)	95.31	67.68 (± 0.48)
	✓	✓	✗	✗	0.37 (± 0.14)	19.53	63.21 (± 0.27)
	✓	✓	✗	P	0.31 (± 0.17)	14.84	57.32 (± 0.19)
	✓	✓	✗	C	0.04 (± 0.02)	0	66.00 (± 0.42)
	✓	✓	✓	✗	0.37 (± 0.13)	16.41	61.51 (± 0.14)
	✓	✓	✓	P	0.25 (± 0.17)	6.25	56.26 (± 0.01)
	✓	✓	✓	C	0.04 (± 0.02)	0	65.38 (± 1.01)

as they implement seminal architectural mechanisms. The ViT uses an embedding patch size 4, 4 transformer blocks with a hidden size 256, 16 attention heads and GELU activation. The ResNet-18 uses the pre-defined architecture as described in the

original paper (He et al. 2016). For both models the final classification layer uses 10 neurons with softmax activation. Additionally, we replace Batch Normalization (BN) layers with Group Normalization (GN) (Wu et al. 2018) as these are the preferred choice in FL scenarios (Hsieh et al. 2020; Zhang et al. 2021). To save computational resources, we focus only on the most promising defense combinations identified in the previous experiments. We include experiments for single defenses for reference. Since GP did not show significant benefits for either privacy or model utility, we exclude it from further consideration.

Table 5. Model utility and privacy metrics for an ablation study using different combinations of defense mechanisms in the ResNet-18 and ViT on the MNIST and CIFAR-10 datasets. We consider Dropout (DO), Differential Privacy (DP), Gradient Pruning (GP) and a Privacy Module (PM) as defense. ✓ and ✕ indicate, whether a defense mechanism was used or not. P and C indicate whether PRECODE or CVB was used, respectively. Arrows indicate direction of improvement from the viewpoint of a defending client. Bold and italic formatting highlight best and worst results, respectively.

		Model	DO	DP	GP	PM	SSIM ↓	ASR [%] ↓	Accuracy [%] ↑
MNIST	ResNet-18	✗	✗	✗	✗	✗	0.51 (± 0.12)	53.91	99.51 (± 0.02)
		✗	✗	✗	✗	P	0.25 (± 0.15)	7.03	99.35 (± 0.04)
		✗	✗	✗	✗	C	0.37 (± 0.12)	14.06	99.46 (± 0.01)
		✗	✓	✗	✗	✗	0.46 (± 0.11)	39.06	99.52 (± 0.04)
		✗	✓	✗	✗	P	0.21 (± 0.11)	0	99.42 (± 0.03)
		✗	✓	✗	✗	C	0.04 (± 0.02)	0	99.54 (± 0.02)
		✓	✗	✗	✗	✗	0.59 (± 0.10)	80.47	99.44 (± 0.01)
		✓	✓	✗	✗	P	0.13 (± 0.07)	0	99.46 (± 0.10)
		✓	✓	✗	✗	C	0.03 (± 0.02)	0	99.52 (± 0.02)
		✗	✗	✗	✗	✗	0.99 (± 0.00)	100	98.84 (± 0.00)
CIFAR-10	ViT	✗	✗	✗	✗	P	0.94 (± 0.03)	100	98.63 (± 0.00)
		✗	✗	✗	✗	C	1.00 (± 0.00)	100	98.95 (± 0.03)
		✗	✓	✗	✗	✗	0.98 (± 0.01)	100	98.85 (± 0.00)
		✗	✓	✗	✗	P	0.02 (± 0.04)	0	98.36 (± 0.00)
		✗	✓	✗	✗	C	0.21 (± 0.06)	0	99.04 (± 0.00)
		✓	✗	✗	✗	✗	0.98 (± 0.02)	100	99.09 (± 0.00)
		✓	✓	✗	✗	P	0.00 (± 0.04)	0	98.81 (± 0.00)
		✓	✓	✗	✗	C	0.13 (± 0.04)	0	98.91 (± 0.00)
		✗	✗	✗	✗	✗	0.55 (± 0.11)	72.66	73.99 (± 0.13)
		✗	✗	✗	✗	P	0.28 (± 0.20)	15.62	74.82 (± 0.27)
CIFAR-10	ResNet-18	✗	✗	✗	✗	C	0.38 (± 0.14)	20.31	74.23 (± 0.57)
		✗	✓	✗	✗	✗	0.55 (± 0.11)	71.09	71.98 (± 0.20)
		✗	✓	✗	✗	P	0.21 (± 0.11)	0	73.25 (± 0.06)
		✗	✓	✗	✗	C	0.06 (± 0.03)	0	71.55 (± 0.23)
		✓	✗	✗	✗	✗	0.63 (± 0.10)	89.84	74.03 (± 0.13)
		✓	✓	✗	✗	P	0.13 (± 0.08)	0	73.27 (± 0.42)
		✓	✓	✗	✗	C	0.06 (± 0.03)	0	72.02 (± 0.28)
		✗	✗	✗	✗	✗	0.90 (± 0.05)	100	63.71 (± 0.00)
		✗	✗	✗	✗	P	0.81 (± 0.07)	100	64.53 (± 0.00)
		✗	✗	✗	✗	C	1.00 (± 0.00)	100	63.44 (± 0.38)
CIFAR-10	ViT	✗	✓	✗	✗	✗	0.86 (± 0.05)	100	61.83 (± 0.43)
		✗	✓	✗	✗	P	0.01 (± 0.02)	0	61.99 (± 0.00)
		✗	✓	✗	✗	C	0.11 (± 0.05)	0	61.31 (± 0.00)
		✓	✗	✗	✗	✗	0.92 (± 0.04)	100	69.47 (± 0.00)
		✓	✓	✗	✗	P	0.01 (± 0.01)	0	69.30 (± 0.00)
		✓	✓	✗	✗	C	0.06 (± 0.03)	0	61.18 (± 0.00)

The results for these experiments are presented in Table 5. The tendencies for model

utility and privacy protection are consistent with the observations made for the CNN. For the ResNet-18, only using a PM (either PRECODE or CVB) already reduces ASR to below 21% for both datasets. DP alone provides a slight reduction in ASR, by 14.85% on MNIST and 1.57% on CIFAR-10. For the ViT, these defenses are insufficient as ASR remains at 100% if only single defenses are applied. For both models and datasets, a combination of DP+PRECODE or DP+CVB is required to reduce ASR to 0%. However, there is no defense combination that consistently delivers the best trade-off between model utility and privacy across all settings. On MNIST, the ResNet-18 and ViT achieve the best trade-off with DP+CVB, reducing ASR to 0% and increasing accuracy by 0.03% and 0.20% compared to the unprotected baseline models, respectively. In contrast, on CIFAR-10, DP+CVB reduces model utility compared to the unprotected baseline. In this case, the best trade-off is achieved with the DO+DP+PRECODE combination, which reduces ASR to 0% for both models. For the ResNet-18, this combination leads to a slight decrease in model utility by 0.72%, while for the ViT, it results in a substantial accuracy increase of 5.59% compared to the baseline model. This improvement is likely due to the positive effect of Dropout on the ViT architecture, which has also been observed in (Scheliga et al. 2023).

7. Conclusion

Privacy preservation in FL is a rapidly evolving field of research that continuously introduces new attacks and enhanced defense mechanisms. First, we adopted an attacker’s perspective to test the limits of commonly applied defense mechanisms. Our findings show that attackers can bypass these defenses by sufficiently approximating and mimicking the client’s stochastic gradient computation process. We implemented three novel targeted attacks and demonstrated that the protection promised by GP, PRECODE, and CVB can be significantly weakened. Ultimately, we found that no individually applied defense mechanism provides adequate privacy protection.

To address this issue, we proposed to combine multiple defenses. Since each defense alters gradient computation in a different way, it becomes increasingly challenging for attackers to fully mimic the gradient computation process and conduct a successful GI attack. We conducted a comprehensive ablation study to evaluate various defense combinations and their impact on both model utility and privacy. To establish an upper bound for privacy leakage, we developed CDIA, an attack specifically targeting each defense applied by the client during local training. Across various scenarios, we found that combining DP with either PRECODE or CVB is essential to protect client privacy, i.e., reducing the ASR to 0%. These combinations also frequently resulted in the highest model utility compared to other defense combinations, single defenses, and even the unprotected baseline. This paper highlights the importance to thoroughly evaluate and analyze defense mechanisms that are supposed to protect client privacy in FL. To this end, we have developed new strategies to more effectively resist privacy threats in collaborative environments.

Funding Details

This work was supported by the Thuringian Ministry of Economics, Science and Digital Society under Grant 5575/10-3.

Disclosure Statement

This paper does not have potential conflict of interest.

Data Availability Statement

All dataset that were used for the experiments are publicly available: MNIST (LeCun et al. 1998); CIFAR-10 (Krizhevsky et al. 2009).

References

Abadi, Martin et al. (2016). “Deep learning with differential privacy”. In: *Proceedings of the 2016 ACM SIGSAC conference on computer and communications security*, pp. 308–318.

Aono, Yoshinori et al. (2017). “Privacy preserving deep learning via additively homomorphic encryption”. In: *IEEE transactions on information forensics and security* 13.5, pp. 1333–1345.

Boenisch, Franziska et al. (2023). “When the curious abandon honesty: Federated learning is not private”. In: *2023 IEEE 8th European Symposium on Security and Privacy (EuroS&P)*. IEEE, pp. 175–199.

Bonawitz, Keith et al. (2017). “Practical secure aggregation for privacy-preserving machine learning”. In: *proceedings of the 2017 ACM SIGSAC Conference on Computer and Communications Security*, pp. 1175–1191.

Deng, Lei et al. (2020). “Model compression and hardware acceleration for neural networks: A comprehensive survey”. In: *Proceedings of the IEEE* 108.4, pp. 485–532.

Dosovitskiy, Alexey et al. (2020). “An image is worth 16x16 words: Transformers for image recognition at scale”. In: *arXiv preprint arXiv:2010.11929*.

Duan, Moming et al. (2019). “Astraea: Self-balancing federated learning for improving classification accuracy of mobile deep learning applications”. In: *2019 IEEE 37th international conference on computer design (ICCD)*. IEEE, pp. 246–254.

Dwork, Cynthia, Aaron Roth, et al. (2014). “The algorithmic foundations of differential privacy”. In: *Foundations and Trends in Theoretical Computer Science* 9.3–4, pp. 211–407.

Fang, Hao et al. (2023). “GIFD: A Generative Gradient Inversion Method with Feature Domain Optimization”. In: *Proceedings of the IEEE/CVF International Conference on Computer Vision*, pp. 4967–4976.

Fowl, Liam et al. (2021). “Robbing the fed: Directly obtaining private data in federated learning with modified models”. In: *arXiv preprint arXiv:2110.13057*.

Fowl, Liam et al. (2022). “Decepticons: Corrupted transformers breach privacy in federated learning for language models”. In: *arXiv preprint arXiv:2201.12675*.

Garov, Kostadin et al. (2023). “Hiding in Plain Sight: Disguising Data Stealing Attacks in Federated Learning”. In: *arXiv preprint arXiv:2306.03013*.

Geiping, Jonas et al. (2020). “Inverting gradients-how easy is it to break privacy in federated learning?” In: *Advances in neural information processing systems* 33, pp. 16937–16947.

Gong, Haimei et al. (2023). “Gradient leakage attacks in federated learning”. In: *Artificial Intelligence Review* 56.Suppl 1, pp. 1337–1374.

Hanson, Stephen José (1990). “A stochastic version of the delta rule”. In: *Physica D: Nonlinear Phenomena* 42.1-3, pp. 265–272.

Hatamizadeh, Ali et al. (2022). “Gradvit: Gradient inversion of vision transformers”. In: *Proceedings of the IEEE/CVF Conference on Computer Vision and Pattern Recognition*, pp. 10021–10030.

He, Kaiming et al. (2016). “Deep residual learning for image recognition”. In: *Proceedings of the IEEE conference on computer vision and pattern recognition*, pp. 770–778.

Hinton, Geoffrey E et al. (2012). “Improving neural networks by preventing co-adaptation of feature detectors”. In: *arXiv preprint arXiv:1207.0580*.

Hsieh, Kevin et al. (2020). “The non-iid data quagmire of decentralized machine learning”. In: *International Conference on Machine Learning*. PMLR, pp. 4387–4398.

Huang, Yangsibo et al. (2021). “Evaluating gradient inversion attacks and defenses in federated learning”. In: *Advances in Neural Information Processing Systems* 34, pp. 7232–7241.

Jayaraman, Bargav and David Evans (2019). “Evaluating differentially private machine learning in practice”. In: *28th USENIX Security Symposium (USENIX Security 19)*, pp. 1895–1912.

Jeon, Jinwoo et al. (2021). “Gradient inversion with generative image prior”. In: *Advances in neural information processing systems* 34, pp. 29898–29908.

Jin, Richeng et al. (2020). “Stochastic-sign SGD for federated learning with theoretical guarantees”. In: *arXiv preprint arXiv: 2002.10940*.

Kairouz, Peter et al. (2021). “Advances and open problems in federated learning”. In: *Foundations and Trends in Machine Learning* 14.1–2, pp. 1–210.

Kingma, Diederik P and Jimmy Ba (2014). “Adam: A method for stochastic optimization”. In: *arXiv preprint arXiv:1412.6980*.

Kingma, Diederik P and Max Welling (2013). “Auto-encoding variational bayes”. In: *arXiv preprint arXiv:1312.6114*.

Krizhevsky, Alex, Geoffrey Hinton, et al. (2009). “Learning multiple layers of features from tiny images”. In.

LeCun, Yann et al. (1998). “Gradient-based learning applied to document recognition”. In: *Proceedings of the IEEE* 86.11, pp. 2278–2324.

Li, Wenqi et al. (2019). “Privacy-preserving federated brain tumour segmentation”. In: *Machine Learning in Medical Imaging: 10th International Workshop, MLMI 2019, Held in Conjunction with MICCAI 2019, Shenzhen, China, October 13, 2019, Proceedings* 10. Springer, pp. 133–141.

Li, Zhaohua et al. (2023). “A survey of image gradient inversion against federated learning”. In: *Authorea Preprints*.

Li, Zhuohang et al. (2022). “Auditing privacy defenses in federated learning via generative gradient leakage”. In: *Proceedings of the IEEE/CVF Conference on Computer Vision and Pattern Recognition*, pp. 10132–10142.

Lin, Yujun et al. (2017). “Deep gradient compression: Reducing the communication bandwidth for distributed training”. In: *arXiv preprint arXiv:1712.01887*.

Liu, Dong C and Jorge Nocedal (1989). “On the limited memory BFGS method for large scale optimization”. In: *Mathematical programming* 45.1, pp. 503–528.

McMahan, Brendan et al. (2017a). “Communication-Efficient Learning of Deep Networks from Decentralized Data”. In: *Artificial intelligence and statistics*. PMLR, pp. 1273–1282.

McMahan, H Brendan et al. (2017b). “Learning differentially private recurrent language models”. In: *arXiv preprint arXiv:1710.06963*.

McMahan, H Brendan et al. (2018). “A general approach to adding differential privacy to iterative training procedures”. In: *arXiv preprint arXiv:1812.06210*.

Mothukuri, Viraaji et al. (2021). “A survey on security and privacy of federated learning”. In: *Future Generation Computer Systems* 115, pp. 619–640.

Pan, Xudong et al. (2022). “Exploring the security boundary of data reconstruction via neuron exclusivity analysis”. In: *31st USENIX Security Symposium (USENIX Security 22)*, pp. 3989–4006.

Ponomareva, Natalia et al. (2023). “How to dp-fy ml: A practical guide to machine learning with differential privacy”. In: *Journal of Artificial Intelligence Research* 77, pp. 1113–1201.

Rao, Bosen et al. (2024). “Privacy Inference Attack and Defense in Centralized and Federated Learning: A Comprehensive Survey”. In: *IEEE Transactions on Artificial Intelligence*.

Ren, Hanchi, Jingjing Deng, and Xianghua Xie (2022). “Grnn: generative regression neural network—a data leakage attack for federated learning”. In: *ACM Transactions on Intelligent Systems and Technology (TIST)* 13.4, pp. 1–24.

Rodríguez-Barroso, Nuria et al. (2023). “Survey on federated learning threats: Concepts, taxonomy on attacks and defences, experimental study and challenges”. In: *Information Fusion* 90, pp. 148–173.

Roy, Abhijit Guha et al. (2019). “Braintorrent: A peer-to-peer environment for decentralized federated learning”. In: *arXiv preprint arXiv:1905.06731*.

Rudin, Leonid I, Stanley Osher, and Emad Fatemi (1992). “Nonlinear total variation based noise removal algorithms”. In: *Physica D: nonlinear phenomena* 60.1-4, pp. 259–268.

Sattler, Felix et al. (2019). “Robust and communication-efficient federated learning from non-iid data”. In: *IEEE transactions on neural networks and learning systems* 31.9, pp. 3400–3413.

Scheliga, Daniel, Patrick Mäder, and Marco Seeland (2022). “PRECODE - A Generic Model Extension to Prevent Deep Gradient Leakage”. In: *Proceedings of the IEEE/CVF Winter Conference on Applications of Computer Vision*, pp. 1849–1858.

- (2023). “Dropout is NOT All You Need to Prevent Gradient Leakage”. In: *Proceedings of the AAAI Conference on Artificial Intelligence*. Vol. 37. 8, pp. 9733–9741.
- (2024a). “Feature-Based Dataset Fingerprinting for Clustered Federated Learning on Medical Image Data”. In: *Applied Artificial Intelligence* 38.1, p. 2394756. DOI: [10.1080/08839514.2024.2394756](https://doi.org/10.1080/08839514.2024.2394756).
- (2024b). “Privacy Preserving Federated Learning with Convolutional Variational Bottlenecks”. In: *Cybersecurity*. Accepted, in press.

Sharma, Anee and Ningrinla Marchang (2024). “A Review on Client-Server Attacks and Defenses in Federated Learning”. In: *Computers & Security*, p. 103801.

Srivastava, Nitish et al. (2014). “Dropout: a simple way to prevent neural networks from overfitting”. In: *The journal of machine learning research* 15.1, pp. 1929–1958.

Tsuzuku, Yusuke, Hiroto Imachi, and Takuya Akiba (2018). “Variance-based gradient compression for efficient distributed deep learning”. In: *arXiv preprint arXiv:1802.06058*.

Wagner, Isabel and David Eckhoff (2018). “Technical privacy metrics: a systematic survey”. In: *ACM Computing Surveys (Csur)* 51.3, pp. 1–38.

Wang, Jiaqi et al. (2022). “In differential privacy, there is truth: on vote-histogram leakage in ensemble private learning”. In: *Advances in Neural Information Processing Systems* 35, pp. 29026–29037.

Wang, Yijue et al. (2020). “Sapag: A self-adaptive privacy attack from gradients”. In: *arXiv preprint arXiv:2009.06228*.

Wang, Zhou et al. (2004). “Image quality assessment: from error visibility to structural similarity”. In: *IEEE transactions on image processing* 13.4, pp. 600–612.

Wei, Wenqi and Ling Liu (2021). “Gradient leakage attack resilient deep learning”. In: *IEEE Transactions on Information Forensics and Security* 17, pp. 303–316.

Wei, Wenqi et al. (2020). “A framework for evaluating client privacy leakages in federated learning”. In: *Computer Security–ESORICS 2020: 25th European Symposium on Research in Computer Security, ESORICS 2020, Guildford, UK, September 14–18, 2020, Proceedings, Part I* 25. Springer, pp. 545–566.

Wen, Yuxin et al. (2022). “Fishing for user data in large-batch federated learning via gradient magnification”. In: *arXiv preprint arXiv:2202.00580*.

Wu, Yuxin and Kaiming He (2018). “Group normalization”. In: *Proceedings of the European conference on computer vision (ECCV)*, pp. 3–19.

Xu, Xiangrui et al. (2022). “CGIR: conditional generative instance reconstruction attacks against federated learning”. In: *IEEE Transactions on Dependable and Secure Computing*.

Yang, Haomiao et al. (2023). “Gradient leakage attacks in federated learning: Research frontiers, taxonomy and future directions”. In: *IEEE Network*.

Yin, Hongxu et al. (2021). “See through gradients: Image batch recovery via gradient-inversion”. In: *Proceedings of the IEEE/CVF Conference on Computer Vision and Pattern Recognition*, pp. 16337–16346.

Zhang, Chi et al. (2023). “Generative Gradient Inversion via Over-Parameterized Networks in Federated Learning”. In: *Proceedings of the IEEE/CVF International Conference on Computer Vision*, pp. 5126–5135.

Zhang, Rui et al. (2022). “A survey on gradient inversion: Attacks, defenses and future directions”. In: *arXiv preprint arXiv: 2206.07284*.

Zhang, Zhengming et al. (2021). “Improving semi-supervised federated learning by reducing the gradient diversity of models”. In: *2021 IEEE International Conference on Big Data (Big Data)*. IEEE, pp. 1214–1225.

Zhao, Bo, Konda Reddy Mopuri, and Hakan Bilen (2020). “iDLG: Improved Deep Leakage from Gradients”. In: *arXiv preprint arXiv:2001.02610*.

Zhu, Junyi and Matthew Blaschko (2021). “R-GAP: Recursive gradient attack on privacy”. In: *Proceedings ICLR 2021*.

Zhu, Ligeng, Zhijian Liu, and Song Han (2019). “Deep leakage from gradients”. In: *Advances in neural information processing systems* 32.